WKB Analysis of Bend Losses in Optical Waveguides

William Berglund and Anand Gopinath

***Abstract*—A more complete Wentzel–Kramers–Brillouin (WKB) analysis of bend losses is given for a circularly curved waveguide. Using the WKB approximation with a conformal transformation of a curved optical waveguide, is shown to give more accurate bend loss results.**

***Index Terms*—Bend losses, dielectric waveguides, Wentzel–Kramers–Brillouin (WKB) method.**

I. Introduction

A NUMBER of methods have been devised for the analysis of losses that occur in curved optical waveguide structures. Heiblum and Harris [1] found that conformally transforming a curved waveguide into a straight structure was a powerful and insightful method of analysis for curved waveguide loss. Using the effective index method (EIM) in the waveguides vertical direction, a two-dimensional (2-D) analysis of the conformally transformed index can be carried out. In their paper, they broke up the transformed region into a series of constant index steps and applied a quantitative geometrical Wentzel–Kramers–Brillouin (WKB) approximation to determine the curvature and transition losses in these guides due to the leaky mode structure of the transformed index.

In this paper, we carry out a more complete WKB analysis of the transformed structure along the lines of analysis by Janta [2], and Gedeon [3]. They found that comparing the calculated mode spectrum by the WKB method for a number of monotonic varying indexes, with the results of numerical calculations showed agreement within 0.03–0.15%. This paper shows a modification of Heiblum-Harris analysis, using the WKB method of [2], [3] shows excellent agreement with experimentally measured waveguide losses; and with other computational intensive methods such as the method of lines (Mol) [4], scalar finite-element (SFEM) [5], vector finite-difference method [6], effective index, and conformal based methods [7], [8].

II. Theory

A curved planar ridge waveguide structure for weakly guided fields can be modeled by the EIM [9] as a curved two-dimensional waveguide structure in the x–y plane. Both TE and TM boundary conditions are used along the dielectric boundaries normal to the z axis, to determine the effective index of the structure with varying thicknesses. Unlike an ideal straight waveguide section where the phase relation for the guided optical field can be maintained, in a curved guide this is not possible as the optical field propagates along the circular curve in the x–y plane. With large curvature each reflection on the outer waveguide boundary, there is some loss of the guided field, the magnitude of this leakage loss is dependent upon the imaginary part of β, the wavevector in the direction of guided wave propagation. The curvature loss for a 90° bend with circular radius of curvature R_2 will be given in decibels by

$$4.342\pi R_2 \,\mathrm{Im}(\beta)\ \mathrm{dB}. \tag{1}$$

For a straight symmetrical slab waveguide the eigenvalue equation for β, with semi-infinite claddings with index n_1, an guide layer with index n_2 and width d, is thus given by the following dispersion relationship:

$$k\sqrt{(n_2^2 - n_3^2)}\,d - 2\phi_1 = n\pi \tag{2a}$$

where the index, $n_3 = (\beta/k)$, k is the freespace wavenumber, and the phase relation

$$\phi_1 = \tan^{-1}\left[S\sqrt{(n_3^2 - n_1^2)/(n_2^2 - n_3^2)}\right]$$

where

$$S = \begin{cases} 1 & \text{TE} \\ \left(\dfrac{n_2}{n_1}\right)^2 & \text{TM} \end{cases}. \tag{2b}$$

Here n_1 and n_2 are the guide indexes as shown in Fig. 1. The roots for the eigenvalue condition (3) are real for guided waves, which implies $\mathrm{Im}(\beta) = 0$, resulting with no loss from (1) for a straight waveguide. It is to be expected that the larger the radius of curvature for a waveguide bend, the closer its eigenvalue condition for β will match the condition given in (2), with a smaller imaginary component of β.

We use the notation E-Mode and M-Mode to denote the transverse electric and transverse magnetic boundary conditions of the propagating optical fields for the two-dimensional boundaries approximation when using EIM, and transverse electric (TE) and transverse magnetic (TM) notation for the boundary conditions that the effective fields satisfy vertically in the ridge structure. The optical fields (E_M, H_M) and (E_E, H_E) in the two-dimensional (2-D) model can be constructed from scalar potentials terms taken from the z components of the respective three-dimensional E and H fields. The WKB bend model of the waveguide is constructed in the following steps listed in Table I.

Here Z_0 is the free space impedance, k is the free space wave number, and n is the effective index of refraction in the x–y plane. The TE and TM boundary conditions are used to find the effective indexes n_{TE} and n_{TM} for the three-dimensional (3-D) ridge structure, these polarizations in the ridge waveguide

Manuscript received December 7, 1999; revised May 10, 2000.

The authors are with the Department of Electrical and Computer Engineering, University of Minnesota, Minneapolis, MN 55455 USA.

Publisher Item Identifier S 0733-8724(00)06478-1.

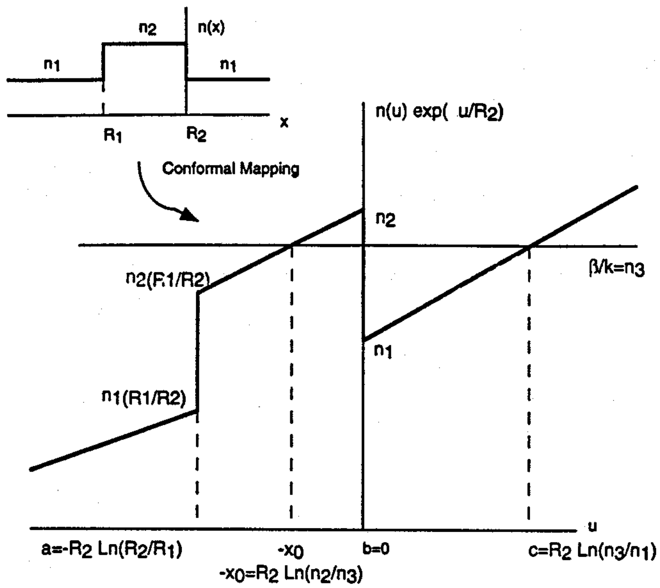

Fig. 1. Conformal mapping of effective index versus transformed transverse u-coordinate.

TABLE I
EIM MODELED RIDGE WAVEGUIDE

1. Vertical Boundary Conditions Ridge Structure	TE Case(a.) Find $n_{TE}(r)$ by EIM	TM Case(b.) Find $n_{TM}(r)$ by EIM
2. Horizontal 2-D Boundary Conditions	M-Mode	E-Mode
3. Electromagnetic Field Equations (3a,b) Fundamental Scalar Fields (Ez and Hz)	$\overline{E}_M = j\dfrac{Z_0(\hat{z}\times\overline{\nabla}_t H_z)}{n_{TE}^2\, k}$ $\overline{H}_M = H_z\,\hat{z}$ $\overline{\nabla}_t\cdot(\frac{1}{n_{TE}^2}\overline{\nabla}_t H_z)+k^2 H_z = 0$ (3a)	$\overline{E}_E = E_z\,\hat{z}$ $\overline{H}_E = -j\dfrac{\hat{z}\times\overline{\nabla}_t E_z}{Z_0\, k}$ $\nabla_t^2 E_z + k^2 n_{TM}^2 E_z = 0$ (3b)

satisfy respective M-Mode and E-Mode polarization boundary conditions in the x–y plane. The vector components E_z and H_z serve as potentials for the fundamental 2-D scalar wave equations in the EIM approximation.

These scalar equations wave (3a) and (3b) can be derived from the following 2-D action integrals [10]:

$$I^E = \int \left(\bar{\nabla}_t E_z^* \cdot \bar{\nabla}_t E_z - k^2 n_{\rm TM}^2 E_z^* E_z\right) dx\, dy \qquad (4a)$$

$$I^M = \int \left(\frac{1}{n_{\rm TE}^2}\bar{\nabla}_t H_z^* \cdot \bar{\nabla}_t H_z - k^2 H_z^* H_z\right) dx\, dy \qquad (4b)$$

where the Action Integrals I^E, and I^M can be expressed as

$$I^E = \int L^E(E_z, E_z^*, \bar{\nabla}_t E_z, \bar{\nabla}_t E_z^*)\, dx\, dy \qquad (5a)$$

$$I^M = \int L^M(H_z, H_z^*, \bar{\nabla}_t H_z, \bar{\nabla}_t H_z^*)\, dx\, dy \qquad (5b)$$

where L^E and L^M are the Lagrangian densities which are functions of E_z and H_z. The equations of motion (3) for the propagating scalar fields can be derived from the following 2-D Euler–Lagrangian equations (6a) and (6b)

$$\frac{\partial L^E}{\partial E_z^*} - \bar{\nabla}_t \cdot \frac{\partial L^E}{\partial(\bar{\nabla}_t E_z^*)} = 0 \qquad (6a)$$

$$\frac{\partial L^E}{\partial H_z^*} - \bar{\nabla}_t \cdot \frac{\partial L^E}{\partial(\bar{\nabla}_t H_z^*)} = 0. \qquad (6b)$$

When the action integrals I^E and I^M remain invariant under proper coordinate and field transformations in the x–y plane, then the Euler–Lagrangian relations (6a), (6b) can be used to find the resulting optical field equations.

Heiblum and Harris [1] found for a two-dimensional waveguide analysis that a simple conformal transformation in the x–y plane could map a circularly curved waveguide into a straight section, resulting in a separable differential equation for (3), given by the following conformal mapping:

$$w = R_2 \ln\left(\frac{z}{R_2}\right), \quad R_2 = \text{Outer Radius of Curvature}$$

where

$$z = x + jy \quad \text{and} \quad w = u + jv. \qquad (7)$$

A Jacobian term from the transformation (7) modifies the effective index of the guide as a function of the u coordinate only

$$J = \frac{\partial(x,y)}{\partial(u,v)} = \left|\frac{dz}{dw}\right|^2 = \exp\left(\frac{2u}{R_2}\right). \qquad (8)$$

However, the conformal transformation of the x–y plane into the complex u–v plane breaks the invariance of the action integral in the potential term in the Lagrangian (4). The key point for the validity of conformal method for a bend loss analysis as done by Heiblum and Harris [1], is that this invariance is approximately invariant in the neighborhood of the waveguiding region, where the Jacobian of the conformal transformation (8) is near unity. The resulting wave equations and boundary conditions for this transformation from the Euler–Lagrangian relations are valid to a good approximation [10], when centered in the region where the coordinate $u \approx 0$, and where $|u| \ll R_2/2$. Further analysis of the conditions and ranges that a conformal transformation is valid, needs to developed, and will be given in a later paper.

Under the conformal transformation in the x–y plane the scalar fields and action integrals transform as follows:

$$\begin{array}{l} E_z \to E_z' = E_z \\ H_z \to H_z' = H_z \end{array} \quad \text{transform as scalar fields} \qquad (9a)$$

$$I^E \to I'^E = \int \left(\bar{\nabla}_t' E_z^* \cdot \bar{\nabla}_t' E_z - k^2 n_{\rm TM}^2 J E_z^* E_z\right) du\, dv \qquad (9b)$$

$$I^M \to I'^M = \int \left(\frac{1}{n_{\rm TE}^2}\bar{\nabla}_t' H_z^* \cdot \bar{\nabla}_t' H_z - k^2 J H_z^* H_z\right) du\, dv. \qquad (9c)$$

With the conformal transformation (7) the circularly curved waveguide is now a straight section, the Euler–Lagrangian equations (6a), (6b) to a good approximation give the following separable differential equations and boundary conditions in the transformed u-v plane where

$$\begin{cases} E_z(u,v) = E_z(u)\exp(-j\beta v) \\ H_z(u,v) = H_z(u)\exp(-j\beta v). \end{cases} \tag{10}$$

E-Mode Case:

$$\frac{d^2E_z}{du^2} + \left(k^2 n_{\mathrm{TM}}^2 \exp\left(\frac{2u}{R_2}\right) - \beta^2\right) E_z = 0. \tag{11a}$$

M-Mode Case:

$$\frac{d}{du}\left(\frac{1}{n_{\mathrm{TM}}^2}\frac{dH_z}{du}\right) + \left(k^2 \exp\left(\frac{2u}{R_2}\right) - \frac{\beta^2}{n_{\mathrm{TE}}^2}\right) H_z = 0. \tag{11b}$$

At a discontinuity $u = u_0$ for $n(u)$, (11a), (11b) satisfy the following boundary conditions:

$$\text{E-Mode}\begin{cases} E_z(u_0)|_-^+ = 0 \\ \left.\dfrac{dE_z(u_o)}{du}\right|_-^+ = 0 \end{cases} \tag{12a}$$

$$\text{M-Mode}\begin{cases} H_z(u_0)|_-^+ = 0 \\ \left.\dfrac{1}{n_{\mathrm{TE}}^2}\dfrac{dH_z(u_o)}{du}\right|_-^+ = 0 \end{cases} \tag{12b}$$

where we define $f(x_o)|_-^+ = f(x_o^+) - f(x_o^-)$, and $f(x_o^+) = \lim_{x\to x_o} f(x)$ for $x > x_o$.

III. WKB Analysis

WKB Method [11] is used to solve the second-order differential equation

$$\frac{d^2\varphi}{dx^2} + k^2(x)\varphi = 0. \tag{13}$$

With the following approximate solutions (see (14a) and (14b) at the bottom of the page). With the requirement that

$$\left|\frac{\pi}{k^2(x)}\frac{dk}{dx}\right| \ll 1 \tag{15}$$

for the WKB approximation to be valid.

Fig. 1 illustrates how the step index change of the curved slab guide is modified under the conformal transformation. Using the equations and boundary conditions derived for the scalar fields under the conformal transformation (11), (12), one can determine the eigenvalue condition for β by the WKB method. Because of the leaky nature of the transformed index for values of the u coordinate greater than $R_2\ln(n_3/n_1)$, the eigenvalue condition for β will have both real and imaginary parts. The imaginary part of β gives the loss due to curvature (1), transition losses can be approximated by (16) for the mode mismatch of fields at junctions between straight and circularly curved sections of waveguide. With a smaller radius of curvature, the maximum of the leaky mode will be shifted more outward with respect to the straight guide, and result in greater mode mismatch and transition loss. Waveguide offsets between straight and curved waveguide sections can be calculated to minimize these losses.

$$\text{Transition Loss(dB)} = 10\log_{10} \times \left(\frac{\left|\int_{-\infty}^{c} E_z^{(1)}(u)E_z^{(2)}(u)\,du\right|^2}{\int_{-\infty}^{c}\left|E_z^{(1)}(u)\right|^2 du \int_{-\infty}^{\infty}\left|E_z^{(2)}(u)\right|^2 du}\right)$$

where

$$c = R_2\ln\left(\frac{n_3}{n_1}\right). \tag{16}$$

For the example of TM polarization in a ridge waveguide, $E_z^1(u)$ is the E-Mode optical potential for the field in the circularly curved waveguide, and $E_z^2(u)$ is defined for the straight waveguide. The upper limit of integration $u = R_2\ln(n_3/n_1)$, in the integral is defined by the outer turning point, where the WKB field becomes radiative in Fig. 1. The integral (16) can be performed numerically by interpolating the WKB fields across the classical turning points as shown in Fig. 2.

The WKB approximation for the fields is acceptable when condition (15) is satisfied, this is true everywhere except for very small values for the radius of curvature R_2, which corresponds to very high loss, and for very large values of the u coordinate. At step discontinuities of the index at points, $a = -R_2\ln(R_2/R_1)$ and $b = 0$ in Fig. 1, a plane wave treatment of the WKB fields (17) in the neighborhood of the point is used [2], see (17a)–(17d) at the bottom of the page. This approximation with the boundary conditions from (12), the WKB connection formula [11] at the turning points $x_0 = -R_2\ln(n_2/n_3)$, and $c = R_2\ln(n_3/n_1)$ with the proper outward radiative boundary conditions (17d), results in the following eigenvalue condition for β:

$$\text{First let } S = \begin{cases} 1 & \text{E-Modes} \\ \left(\dfrac{n_2}{n_1}\right)^2 & \text{M-Modes} \end{cases} \tag{18}$$

and define $n_3 = \beta/k$, and waveguide width $d = R_2 - R_1$.

$$\varphi \approx \begin{cases} \dfrac{1}{\sqrt{k(x)}}\exp\left(\pm j\displaystyle\int_a^x k(\varepsilon)\,d\varepsilon\right) & \text{if } k^2(x) > 0 \qquad (14a) \\ \dfrac{1}{\sqrt{\kappa(x)}}\exp\left(\pm\displaystyle\int_a^x \kappa(\varepsilon)\,d\varepsilon\right) & \text{if } k^2(x) < 0, \quad \text{and} \quad k^2(x) = -\kappa^2(x) \qquad (14b) \end{cases}$$

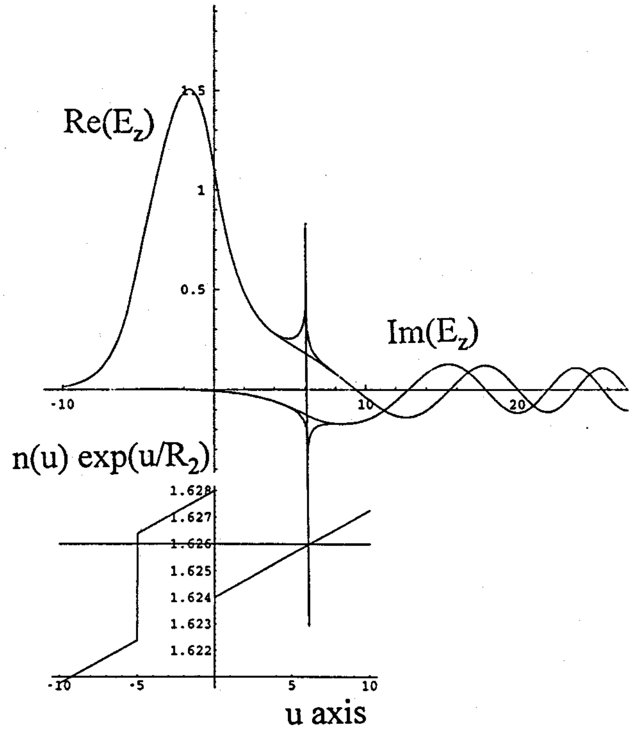

Fig. 2. Interpolated WKB field with conformal bend index versus transverse u-coordinate.

Then define integral (see (19a) and (19b) at the bottom of the next page.)

A. WKB Eigenvalues Condition

$$\tan(\tilde{K}-\phi_1)=S\sqrt{\frac{(n_3^2-n_1^2)}{(n_2^2-n_3^2)}}\,\frac{\left(1+\frac{j}{2}\exp(-2\Gamma_{bc})\right)}{\left(1-\frac{j}{2}\exp(-2\Gamma_{bc})\right)}. \quad (20)$$

For

$$n_3\leq\frac{R_1}{R_2}n_2,\quad \tilde{K}=K_{ab} \quad (21a)$$

inner phase term

$$\phi_1=\tan^{-1}\left[S\sqrt{\frac{\left(n_3^2-n_1^2\left(\frac{R_1}{R_2}\right)^2\right)}{\left(n_2^2\left(\frac{R_1}{R_2}\right)^2-n_3^2\right)}}\right]. \quad (21b)$$

For the whispering gallery mode case

$$n_3>\frac{R_1}{R_2}n_2,\quad \tilde{K}=K_{ax_0} \quad (22a)$$

and

$$\phi_1=\frac{\pi}{4}+\tan^{-1}\left[\frac{1}{2}\left(\frac{S-\chi}{S+\chi}\right)\exp(-2\Gamma_{ax_0})\right]$$

where

$$\chi=\sqrt{\frac{\left(n_3^2-n_2^2\left(\frac{R_1}{R_2}\right)^2\right)}{\left(n_3^2-n_1^2\left(\frac{R_1}{R_2}\right)^2\right)}}. \quad (22b)$$

The main difference of the eigenvalue condition given in (20) from the results given in [1] is in the imaginary loss term. An expansion of the WKB eigenvalue condition given in terms of the tunneling integral Γ_{bc} (19b), gives a smaller attenuation term than from the result given in [1], by a factor of one half. The WKB eigenvalue condition for large radius of curvature reduces to the straight waveguide eigenvalue condition (2). The phase term (21b) for the whispering gallery case is more complete when $n_3>(R_1/R_3)n_2$, accounting for the effects of the buried inner boundary at $a=-R_2\ln(R_2/R_1)$ for the curved guide.

$$E_z(u,v)=e^{-j\beta v}\begin{cases}\dfrac{A\exp\left(-\int_u^a\kappa_{\mathrm{I}}(\varepsilon)\,d\varepsilon\right)}{\sqrt{\kappa_{\mathrm{I}}(u)}} & \text{for } u<a \quad (17a)\\ \dfrac{B\cos\left(\int_a^u k_{\mathrm{II}}(\varepsilon)\,d\varepsilon-\phi\right)}{\sqrt{k_{\mathrm{II}}(u)}} & \text{for } a<u<b \quad (17b)\\ \dfrac{C\exp\left(-\int_b^u\kappa_{\mathrm{I}}(\varepsilon)\,d\varepsilon\right)}{\sqrt{\kappa_{\mathrm{I}}(u)}}+\dfrac{D\exp\left(\int_b^u\kappa_{\mathrm{I}}(\varepsilon)\,d\varepsilon\right)}{\sqrt{\kappa_{\mathrm{I}}(u)}} & \text{for } b<u<c \quad (17c)\\ \dfrac{E\exp\left(-j\int_c^u k_{\mathrm{I}}(\varepsilon)\,d\varepsilon\right)}{\sqrt{k_{\mathrm{I}}(u)}} & \text{for } u>c \text{ outgoing wave} \quad (17d)\end{cases}$$

$$\begin{cases}K_{xy}=\displaystyle\int_x^y k(u)\,du,\quad \text{and}\quad k(u)=k\sqrt{n^2(u)\exp\left(\frac{2u}{R_2}\right)-n_3^2} & (19a)\\ \Gamma_{xy}=\displaystyle\int_x^y \kappa(u)\,du,\quad \text{and}\quad \kappa(u)=k\sqrt{n_3^2-n^2(u)\exp\left(\frac{2u}{R_2}\right)} & (19b)\end{cases}$$

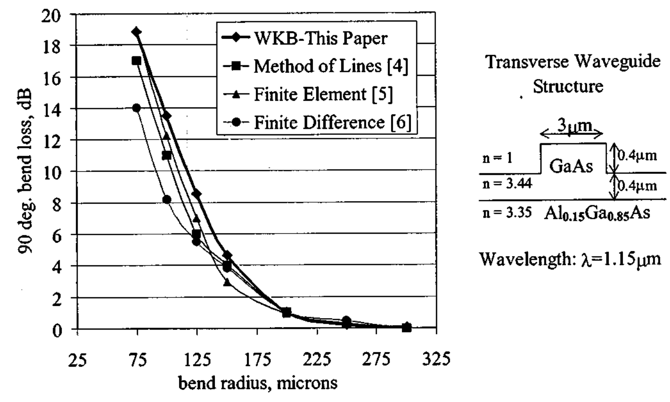

Fig. 3. Comparsion of bend loss methods versus bend radius.

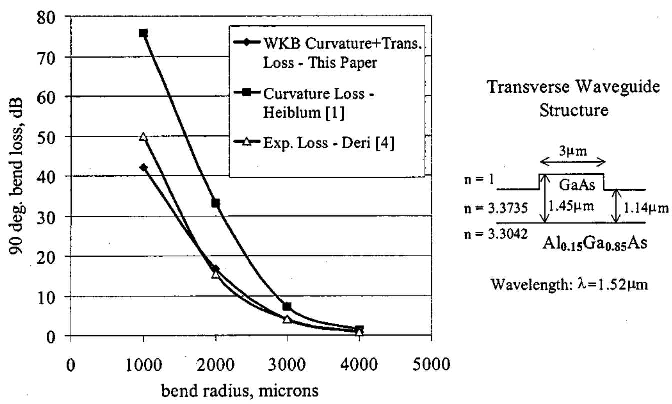

Fig. 4. WKB and experimental bend loss result versus bend radius.

The phase discontinuity of the fields at the point between conditions (21), (22) has been greatly improved from [1], a reduced phase discontinuity still occurs at this point due to a small error in using the connection formulas with more than one WKB solution present [11].

IV. Examples

The eigenvalues from (16) can be determined by graphical means by computer programs such as Mathematica. WKB fields have singularities at turning points, however one can use the validity condition (15) to setup matching conditions to interpolate the fields across these regions, in order to perform transition loss calculations. Comparison of bend losses from the WKB eigenvalue condition (16) with other theoretical methods [4]–[8] in Fig. 3 shows good agreement. For instance, in Fig. 4 the WKB results given in this paper shows better agreement than [1] for the calculated curvature and transition losses in (13), (16), to the experimental results for bend losses from a TE polarized curved GaAs–AlGaAs ridge guide [12].

V. Conclusion

A WKB analysis of losses from curved waveguide by conformal transformation shows excellent agreement with experimental and other more computational intensive methods, better than what has been presented previously by this method. A relatively simple graphical method can be used to quickly determine the roots for the eigenvalue condition for β, and the WKB fields can be interpolated to allow overlap integral calculations for transition losses and offset.

Appendix

The WKB Method relies on connection formulas [11] to match the asymptotic form of the solutions of (19) in the region of the turning points where $k^2(x) = 0$, to (20a) and (20b)

$$\frac{2\cos\left(\int_x^a k(\varepsilon)\,d\varepsilon - \frac{\pi}{4}\right)}{\sqrt{k(x)}} \leftrightarrow \frac{\exp\left(-\int_a^x \kappa(\varepsilon)\,d\varepsilon\right)}{\sqrt{\kappa(x)}} \tag{23a}$$

$$\frac{\sin\left(\int_x^a k(\varepsilon)\,d\varepsilon - \frac{\pi}{4}\right)}{\sqrt{k(x)}} \leftrightarrow \frac{-\exp\left(\int_a^x \kappa(\varepsilon)\,d\varepsilon\right)}{\sqrt{\kappa(x)}}. \tag{23b}$$

The integrals in (15a) and (15b) have the following closed-form solutions:

$$K_{xy} = \int_x^y k_0\sqrt{n_2^2\exp\left(\frac{2u}{R_2}\right) - n_3^2\,du} \tag{19a}$$

$$\begin{aligned} &= k_0R_2\left(\sqrt{n_2^2\exp\left(\frac{2y}{R_2}\right) - n_3^2}\right.\\ &\quad - \sqrt{n_2^2\exp\left(\frac{2x}{R_2}\right) - n_3^2}\\ &\quad - n_3\left(\cos^{-1}\left(\frac{n_3}{n_2}\exp\left(-\frac{y}{R_2}\right)\right)\right.\\ &\quad \left.\left. - \cos^{-1}\left(\frac{n_3}{n_2}\exp\left(-\frac{x}{R_2}\right)\right)\right)\right) \end{aligned} \tag{24a}$$

$$\Gamma_{xy} = \int_x^y k_0\sqrt{n_3^2 - n_2^2\exp\left(\frac{2u}{R_2}\right)}\,du \tag{19b}$$

$$\begin{aligned} &= k_0R_2\left(\sqrt{n_3^2 - n_2^2\exp\left(\frac{2y}{R_2}\right)}\right.\\ &\quad - \sqrt{n_3^2 - n_2^2\exp\left(\frac{2x}{R_2}\right)}\\ &\quad - n_3\left(\ln\left(\frac{n_3}{n_2}\exp\left(-\frac{y}{R_2}\right)\right.\right.\\ &\quad \left. + \sqrt{\left(\frac{n_3}{n_2}\exp\left(-\frac{y}{R_2}\right)\right)^2 - 1}\right)\\ &\quad - \ln\left(\frac{n_3}{n_2}\exp\left(-\frac{x}{R_2}\right)\right.\\ &\quad \left.\left.\left. + \sqrt{\left(\frac{n_3}{n_2}\exp\left(-\frac{x}{R_2}\right)\right)^2 - 1}\right)\right)\right). \end{aligned} \tag{24b}$$

REFERENCES

[1] M. Heiblum and J. H. Harris, "Analysis of curved waveguides by conformal transformation," *IEEE J. Quantum Electron.*, vol. QE-11, pp. 75–83, 1975.

[2] J. Janta and J. Ctyroky, "On the accuracy of WKB analysis of TE and TM modes in planar graded-index waveguides," *Opt. Commun.*, vol. 25, pp. 49–52, 1978.

[3] A. Gedeon, "Comparison between rigorous theory and WKB-analysis of modes in graded-index waveguides," *Opt. Commun.*, vol. 12, pp. 329–332, 1974.

[4] J. Gu, P. Besse, and H. Melchior, "Novel method for analysis of curved optical rib-waveguides," *Electron. Lett.*, vol. 25, pp. 278–280, 1989.

[5] T. Yamamoto and M. Koshiba, "Numerical analysis of curvature loss in optical waveguides by finite-element method," *J. Lightwave Technol.*, vol. 11, pp. 1579–1583, 1993.

[6] S. Kim and A. Gopinath, "Vector analysis of optical dielectric waveguide bends using finite-difference method," *J. Lightwave Technol.*, vol. 14, pp. 2085–2092.

[7] K. Thyagarajan, M. R. Shenoy, and A. K. Ghatak, "Accurate numerical method for the calculation of bending loss in optical waveguide using a matrix approach," *Opt. Lett.*, vol. 12, pp. 296–298, 1987.

[8] D. Rowland, "Nonperturbative calculation of bend loss for a pulse in a bent planar waveguide," *Inst. Elec. Eng. Proc.—Optoelectron.*, vol. 144, pp. 91–96, 1997.

[9] E. A. Marcatili, "Dielectric rectangular waveguide and directional coupler for integrated optics," *Bell Syst. Tech. J.*, vol. 48, pp. 2071–2102, 1969.

[10] R. Wu and C. H. Chen, "A scalar variational conformal mapping technique for weakly guiding dielectric waveguides," *IEEE J. Quantum Electron.*, vol. Qe-22, pp. 603–609, 1986.

[11] D. Bohm, *Quantum Theory*. Englewood Cliffs, NJ: Prentice-Hall, 1951, ch. 12.

[12] R. Deri, E. Kapon, and L. Schiavone, "Bend losses in GaAs/AlGaAs optical waveguides," *Electron. Lett.*, vol. 23, pp. 845–847, 1987.

William Berglund, photograph and biography not available at the time of publication.

Anand Gopinath, photograph and biography not available at the time of publication.